The small tight aspect ratio tokamak experiment

R. J. Colchin, P. G. Carolan, R. Duck, T. Edlington, S. K. Erents et al.

Citation: Phys. Fluids B **5**, 2481 (1993); doi: 10.1063/1.860732
View online: http://dx.doi.org/10.1063/1.860732
View Table of Contents: http://pop.aip.org/resource/1/PFBPEI/v5/i7
Published by the American Institute of Physics.

The Small Tight Aspect Ratio Tokamak experiment*

R. J. Colchin,[†,a)] P. G. Carolan, R. Duck,[b)] T. Edlington, S. K. Erents, J. Ferreira, S. J. Fielding, K. Gibson,[b)] D. H. J. Goodall, M. Gryaznevich, T. C. Hender, J. Hugill, I. Jenkins, J. Li, S. J. Manhood, B. J. Parham, D. C. Robinson, M. Singleton, A. Sykes, T. N. Todd, M. F. Turner, M. Valovic, M. Walsh, and H. R. Wilson

AEA Fusion Technology, Culham Laboratory (EURATOM/UKAEA Association), Abingdon, Oxon, England

(Received 30 November 1992; accepted 15 February 1993)

Low-aspect-ratio tokamaks offer both the economic advantage of smaller size and a number of physics advantages which are not available at conventional aspect ratio. The Small Tight Aspect Ratio Tokamak (START) [*Fusion Technology 1990,* edited by B. E. Keen, M. Huguet, and R. Hemsworth (North-Holland, Amsterdam, 1991), Vol. 1, p. 353] was conceived as a first substantial test of tokamak plasma behavior at low aspect ratio. It has achieved plasma currents up to 200 kA, peak densities of $\sim 2\times 10^{20}$ m^{-3} and central electron temperatures of ~ 500 eV at an aspect ratio of 1.3–1.5. Central beta values of $\sim 13\%$ have been measured and the volume-averaged beta $\langle\beta\rangle$ can approach the Troyon limit. Plasmas are naturally elongated ($\kappa \lesssim 2.0$) and are vertically stable without feedback control. Major disruptions have not been observed at low aspect ratios ($A \leqslant 2.0$).

I. INTRODUCTION

Low-aspect-ratio tokamak plasmas have been predicted[1,2] to have a number of projected physics advantages, several of which could prove crucial for the successful achievement of fusion power production. The Small Tight Aspect Ratio Tokamak (START)[3] is the first tokamak to obtain hot plasmas at an aspect ratio below 2.0.[1] Data from the START device are beginning to confirm several of these predictions. For example, very high beta is possible at low aspect ratio as large plasma currents can be obtained at low toroidal field. Since Ohmic heating can be more effective at low aspect ratio because the fraction of trapped particles is higher, it may be possible to obtain these high beta plasmas without additional heating.

Low-aspect-ratio plasmas are naturally elongated[1] and enjoy good vertical stability properties. START plasmas are vertically stable in the absence of feedback control and have been surprisingly[4] stable to major disruptions, perhaps due to the high edge q_a and high edge shear typical of low aspect ratio. The magnetic islands have been calculated to become narrower as the aspect ratio decreases.[5]

The cross-sectional area of the central tokamak "core" must be small in low-aspect-ratio tokamaks. In large devices such as future reactors, this precludes the incorporation of a high-flux transformer, and so noninductive current drive will be necessary. This is not really a restriction for steady-state devices, since transformer current drive is limited. The inductance of a low-aspect-ratio tokamak is low, implying low volt-second requirements to reach a specified current. However, having obtained that current, the higher resistance caused by trapped electrons acts to increase the voltage whereas the bootstrap current[6] acts to reduce it. High bootstrap and diamagnetic current fractions are predicted in some reactor scenarios,[7] minimizing requirements for auxiliary current drive.

There are also a number of possible economic advantages to low-aspect-ratio operation, the principal being that appreciably smaller tokamaks can be built.[8] This may be particularly important in the near term for constructing a plasma neutron source[9] or a pilot plant.[10]

II. START EXPERIMENTAL SETUP

The START device[3] (see Fig. 1) consists of a large (2 m diam by 2 m tall) cylindrical vacuum chamber which houses the Ohmic heating and vertical field coils. The plasma is initially induced at large minor radius and is compressed toward the center column.[4,11,12] Currents up to 220 kA (peak current) have been created by this technique, although most of the data from START have been taken at 100 kA. In addition, a small Ohmic heating (OH) transformer (~ 8 mV·sec) is wound around the center post. Current is applied to this coil after the plasma is compressed in order to provide a current "flattop" of a few milliseconds duration. The toroidal magnetic field circuit consists of a pulse transformer which feeds current to a solid copper central rod. It is connected in parallel to eight copper return limbs just outside the vacuum chamber, which return the current to the pulse transformer. The center rod current most often used is 480 kA, giving toroidal magnetic field of 0.48 T at a radius of 20 cm. All coils are powered by capacitor banks. The central rod is surrounded by a stainless steel vacuum jacket and is further protected by a graphite limiter in the vicinity of the plasma. The diameter of the rod–OH winding–jacket–limiter combination is 10 cm.

*Paper 1I5, Bull Am. Phys. Soc. **37**, 1354 (1992).

[†]Invited speaker.

[a)]Permanent address: Oak Ridge National Laboratory, Oak Ridge, Tennessee 37831.

[b)]Department of Pure and Applied Physics, UMIST, Manchester, England.

 0899-8221/93/5(7)/2481/4/$6.00

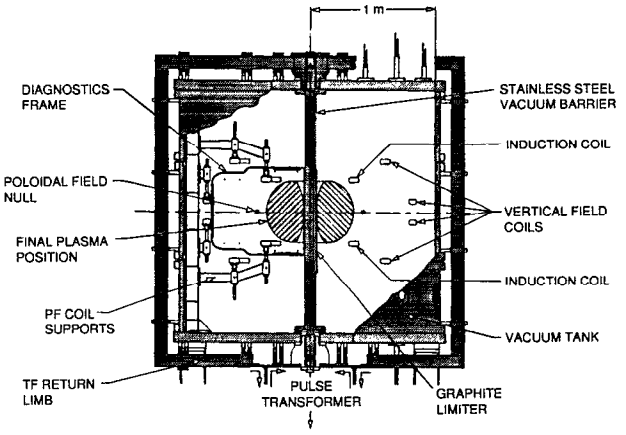

FIG. 1. Schematic of the START apparatus, including the poloidal and toroidal field coils. The plasma is shown at minimum aspect ratio, after compression.

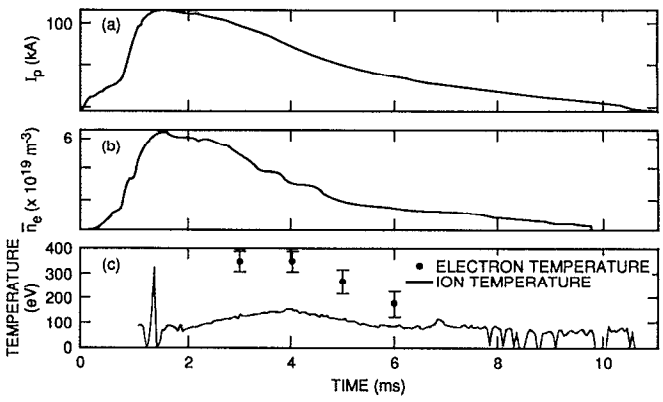

FIG. 2. Plasma parameters as a function of time: (a) plasma current; (b) line-integral density; and (c) ion temperature measured by a neutral particle analysis and electron temperature measured by a soft x-ray spectrometer.

The diagnostics available include Thomson scattering, a 337 μm microwave interferometer, a neutral particle analyzer, a scannable Si(Li) soft x-ray spectrum analyzer, a bolometer, both linear and two-dimensional charge-coupled device (CCD) cameras, two soft x-ray arrays, two visible monochrometers, a vacuum polychrometer and a high-resolution spectrometer, Langmuir probes, numerous magnetic loops (pickup coils, flux loops, and Rogowski coils), and a high-speed cinefilm camera. Several of the pickup loops are installed in the graphite limiter surrounding the central column. There are four gas puff valves close to the plasma formation region for gas-injection control.

III. PLASMA RESULTS

A range of START plasma parameters is listed in Table I. The aspect ratio is lowest following compression when the plasma radius is largest (0.18–0.22 m), being as low as 1.3. After reaching a peak, the plasma current decays, and the plasma decreases in size and increases in aspect ratio. The elongation of the low-aspect-ratio plasma is typically 1.2–1.6, dependent upon the applied vertical field and the plasma current profile. Immediately following internal reconnections it can temporarily rise to $\sim$2.0.

Figure 2 gives the time history of the density, the ion and electron temperatures, and plasma current for a typical 100 kA shot. As shown in Fig. 2(c), the plasma electron and ion temperature increase for $\sim$2 msec after compression (i.e., after the peak in the plasma current). Following compression, the ion temperature ramps up from $\sim$50 to $\sim$140 eV. The ion temperature then decays with a time constant of $\sim$3.5 msec.

The ratio of the initial (before compression in major radius) to final (low aspect ratio) plasma current can be varied by choice of the vertical fields applied to compress the plasma, and this enables a range of plasma conditions to be produced. Figure 3 compares electron temperature profiles measured by a Thomson scattering diagnostic for three types of 100 kA discharges. Each profile was taken at approximately 3.5 msec after initiation of the discharge. The highly compressed discharges [curve (a) in Fig. 3] can attain electron temperatures in excess of 500 eV, and have aspect ratios $A \sim 1.5$. Further details of the moderately

TABLE I. START parameters.

Major radius R, m	0.18–0.22
Minor radius a, m	0.13–0.17
Aspect ratio A	1.3–1.5
Elongation κ	>1.3
Triangularity δ	0.2–0.4
Plasma current I_p, kA	60–200
Toroidal field B_0, T	0.4–0.6
Safety factor q_a	6–15
Pulse duration, msec	$\lesssim 18$
Peak electron density n_e, m^{-3}	$\leqslant(2\text{–}3)\times 10^{20}$
Peak electron temperature T_e, eV	300–500
Ion temperature T_i, eV	100–500
Energy confinement time τ_E, msec	2–3 (at 100 kA)
Resistivity enhancement factor (above Spitzer)	~ 3
Z_{eff}	~ 2 (at 100 kA)

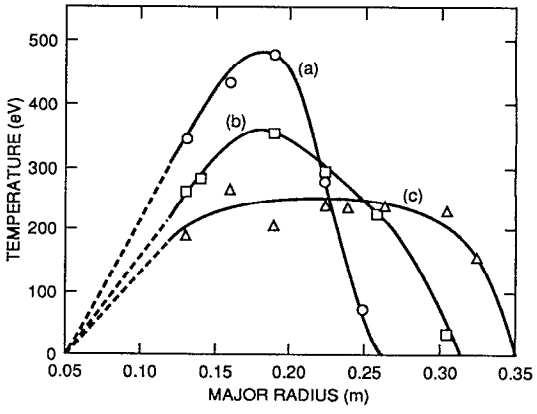

FIG. 3. Electron temperature profiles measured at $t=3.5$ msec for three types of discharges: (a) highly compressed; (b) moderately compressed; and (c) less compressed.

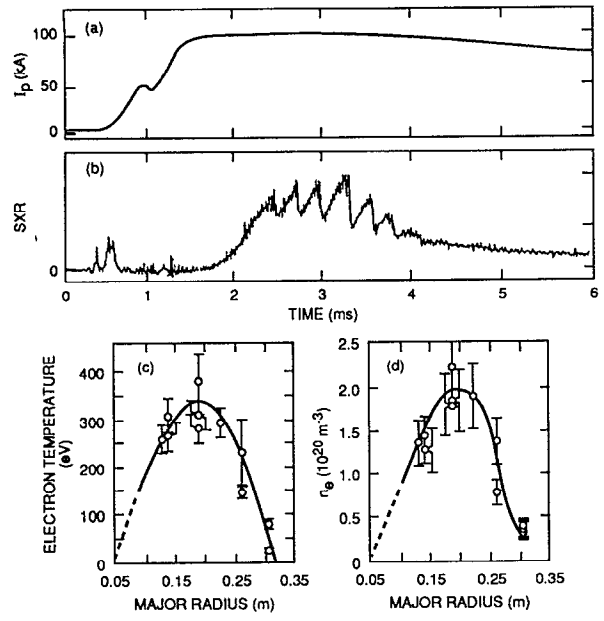

FIG. 4. A discharge with moderate compression: (a) plasma current; (b) soft x-ray signal at $R=0.19$ m, arbitrary units; (c) $T_e(r)$; and (d) $n_e(r)$ profiles at $t=3.5$ msec.

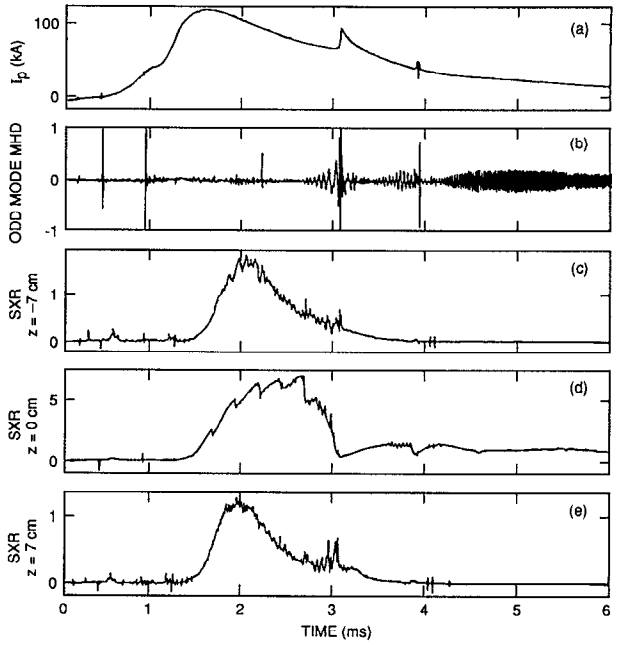

FIG. 5. MHD characteristics of a START discharge: (a) plasma current; (b) odd mode MHD activity recorded by subtracting the signal from two pickup coils separated by 180°; (c) signal from a soft x-ray diode aimed horizontally at $z=-7$ cm; (d) signal from a soft x-ray diode aimed along the midplane; and (e) signal from a soft x-ray diode aimed at $z=+7$ cm.

compressed [Fig. 3, curve (b)] discharges are given in Fig. 4 and show a combination of high temperature and very high density. This produces high beta values, estimated at 13% (central) and 2.6% (volume average, $2\mu_0\langle p\rangle/B_0^2$) compared to a Troyon value ($2.8I_p/aB_0$) of 4%. These plasmas have aspect ratio $A\sim 1.4$.

The less compressed, larger but colder [Fig. 3, curve (c)] discharges also have high beta, 2.5% compared to a Troyon limit of 3.9%, and for these discharges the confinement time is estimated to be $\tau_E=(2.8\pm 0.5)$ msec, compared to predictions of 1.7, 2.7, and 1.5 msec, respectively, from neo-Alcator ($\tau_E=0.7\bar{n}aR^2q^*$), Rebut–Lallia, and T-10 scaling laws. The poloidal beta [$B_I=8\pi\int p\,dS/(\mu_0 I^2)$] is 0.52. Note that these values are achieved by Ohmic heating alone. The aspect ratio of these plasmas is 1.33 and the plasma elongation observed by optical diagnostics is 1.6.

Various types of MHD (magnetohydrodynamic) activity are evident in START discharges.[13] Sawteeth are clearly observed near the plasma center, as shown by the soft x-ray diodes observing the plasma at $z=-7$ cm, 0, and $+7$ cm, Figs. 5(c)–5(e); see also Fig. 4(b). These sawteeth are relatively small in amplitude but demonstrate the existence of central $q<1$ surfaces as do the occasional observation of "snakes." The MHD modes $n=1$, $m=0$, 1, 2, and 3 have been found. Occasionally a steady Mirnov oscillation is observed, as shown near the end of the discharge in Fig. 5(b). Several internal reconnections are also seen on this trace. Sometimes these reconnections are preceded by Mirnov oscillations, such as those occurring before the reconnection at 3.1 msec. Reconnections cause the current profile to become flatter, decreasing the internal plasma inductance and increasing the plasma elongation. This decrease in inductance causes the current to rise, as shown in the current trace at 3.1 msec, Fig. 5(a).

Although current spikes associated with internal reconnections may be quite large (due to the high ratio of the internal to the external inductance), they do not cause current-terminating major disruptions of the plasma when the aspect ratio $A\leqslant 2.0$. If too much gas is fed into the plasma by increasing the filling pressure, a large-scale surface kink mode is observed. If the plasma is subjected to an increase in vertical field which drives it into the central limiter, it will typically undergo successive internal disruptions (i.e., reconnections) until it has decreased in size and its aspect ratio is greater than 2.0, after which a major disruption may occur. The observed absence of major disruptions at $A\leqslant 2.0$ may be attributed to several factors: (1) high edge q_a, (2) high edge shear, (3) smaller island size and a broad spectrum of modes due to higher toroidicity, and (4) lack of plasma-limiter contact except at the center column.

The plasma exhaust in START differs from that in high-aspect-ratio tokamaks because of differences in magnetic geometry. START's poloidal flux is shown in Fig. 6. The region labeled 1 is analogous to the scrape-off layer of plasmas which lean on the inner wall of conventional tokamaks. High edge q_a implies that the magnetic field connection length is moderately long. The region labeled 2 in Fig. 6 corresponds with the exhaust plume observed in optical photographs and can have very long connection lengths to an "extended limiter." It is unique to low aspect ratio. In START the magnetic flux lines in region 2 are prematurely terminated by graphite limiters on the diagnostic frames. An array of Langmuir probes is located in

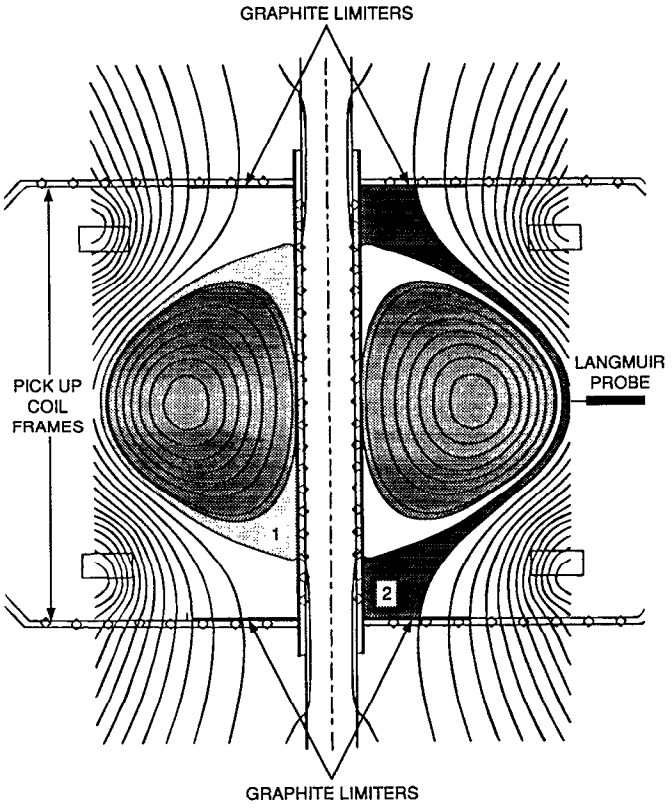

FIG. 6. Schematic of the START plasma exhaust system showing the plasma, the exhaust region inside the separatrix (labeled "1" in the figure), and the plasma exhaust outside the separatrix (labeled "2" in the figure).

the vicinity of the limiters. The flux surfaces are close together at the edge of the plasma at the midplane, and Langmuir probe measurements show that a considerable fraction of the power flowing from the plasma reaches region 2. They also show steep temperature and density gradients at the last closed flux surface.

IV. PRINCIPAL RESULTS—SUMMARY

The START experiment has demonstrated naturally elongated plasmas that are vertically stable up to elongations of ~ 2. The magnetic geometry of low aspect ratio confers a unique plasma exhaust system with long connection lengths. Energy confinement times have been found to exceed the more pessimistic R^2-type predictions of scaling laws such as neo-Alcator. Peak betas of $\sim 13\%$ have been achieved in Ohmically heated plasmas, with average betas that approach the Troyon limit. No major disruptions at aspect ratio $\leqslant 2.0$ have been observed in over 12 000 discharges.

ACKNOWLEDGMENTS

This work was funded jointly by the United Kingdom (U.K.) Department of Trade and Industry, EURATOM, and under Subcontract No. 35YSK923V with AEA (Atomic Energy Authority) Fusion by Martin Marietta Energy Systems, Inc., under Contract No. DE-AC05-84OR21400 with the U.S. Department of Energy.

[1] Y.-K. M. Peng and D. J. Strickler, Nucl. Fusion **26**, 769 (1986).
[2] J. A. Holmes, L. A. Charlton, J. T. Hogan, B. A. Carreras, and E. A. Lazarus, Phys. Fluids B **1**, 358 (1989).
[3] R. T. C. Smith, J. A. Booth, G. Cunningham, E. Del Bosco, J. B. Hicks, D. C. Robinson, A. Sykes, T. N. Todd, and B. J. Ward, in *Fusion Technology 1990*, edited by B. E. Keen, M. Huguet, and R. Hemsworth (North-Holland, Amsterdam, 1991), Vol. 1, p. 353.
[4] A. Sykes, E. Del Bosco, R. J. Colchin, G. Cunningham, R. Duck, T. Edlington, D. H. J. Goodall, M. P. Gryaznevich, J. Holt, J. Hugill, J. Li, S. J. Manhood, B. J. Parham, D. C. Robinson, T. N. Todd, and M. F. Turner, Nucl. Fusion **32**, 694 (1992).
[5] B. A. Carreras, L. A. Charlton, J. T. Hogan, W. A. Cooper, and T. C. Hender, in *Plasma Physics and Controlled Nuclear Fusion Research*, Kyoto, 1986 (International Atomic Energy Agency, Vienna, 1987), Vol. 2, p. 53.
[6] H. R. Wilson, Nucl. Fusion **32**, 257 (1992).
[7] T. C. Hender, L. J. Baker, R. Hancox, J. B. Hicks, P. J. Knight, D. C. Robinson, and H. R. Wilson, in *Plasma Physics and Controlled Nuclear Fusion Research*, Würzburg, 1992 (International Atomic Energy Agency, Vienna, in press), Paper IAEA-CN-56/G-2-5.
[8] Y.-K. M. Peng and J. B. Hicks, in Ref. 3, Vol. 2, p. 1287.
[9] Y.-K. M. Peng, J. D. Galambos, and P. C. Shipe, Fusion Technol. **21**, 1729 (1992).
[10] S. O. Dean, C. C. Baker, J. Galambos, Y.-K. M. Peng, J. Sheffield, D. P. Dautovich, W. G. Morison, W. R. Ellis, and B. B. Kadomtsev, in Ref. 7, Paper IAEA-CN-56/G-1-5.
[11] A. Sykes, "Behavior of low-aspect-ratio tokamak plasmas," Plasma Phys. Controlled Fusion. **34**, 1925 (1992).
[12] M. Gryaznevich, M. Bondeson, P. Carolan, G. Cunningham, R. Duck, T. Edlington, S. K. Erents, J. Ferreira, S. J. Fielding, K. Gibson, D. H. J. Goodall, T. C. Hender, J. Hugill, I. Jenkins, J. Li, S. J. Manhood, A. Nicolai, B. J. Parham, D. C. Robinson, M. Singleton, A. Sykes, T. N. Todd, M. F. Turner, M. Valovic, and M. Walsh, in Ref. 7, Paper IAEA-CN-56/C-3-6(C).
[13] M. Gryaznevich, M. Bondeson, R. Duck, T. C. Hender, D. C. Robinson, and A. Sykes, in *Controlled Fusion and Plasma Physics 1992*, Proceedings of the 19th European Conference, Innsbruck (European Physical Society, Geneva, 1992), Vol. 16C, Part I, p. 399.